Chemical Science

ROYAL SOCIETY OF CHEMISTRY

EDGE ARTICLE

View Article Online
View Journal | View Issue

Check for updates

Cite this: *Chem. Sci.*, 2025, **16**, 9943

All publication charges for this article have been paid for by the Royal Society of Chemistry

Received 14th January 2025
Accepted 23rd April 2025

DOI: 10.1039/d5sc00341e

rsc.li/chemical-science

α-*N*-phthalimido-oxy isobutyrate-mediated deoxygenative arylation: total synthesis of alanenses A and B†

Young Eum Hyun, [a] Jeonguk Kweon, [ba] Thi Hieu Linh Phan, [a] Dongwook Kim [ba] and Sunkyu Han [*ab]

Inspired by a biosynthetic hypothesis of alanense A, we developed two distinct methods for the deoxygenative arylation of α-*N*-phthalimido-oxy isobutyrate (NPIB), derived from hydroxyl groups adjacent to or conjugated with a carbonyl moiety. One approach utilizes photoredox catalysis to achieve a radical-mediated arylation reaction. The other approach involves an acid-mediated arylation method that proceeds through a cationic intermediate. The acid-mediated approach was successfully applied to the total syntheses of alanenses A, B, and O7′-methyllacinilene E.

Introduction

Two-phase biosynthesis of terpene natural products, encompassing a cyclization phase followed by an oxidation phase, is a well-established process.[1,2] Cadinane sesquiterpenoids conform to this paradigm. The cadinane framework, biosynthesized *via* the cyclization of farnesyl pyrophosphate, undergoes biosynthetic oxidations, resulting in remarkable structural diversity.[3,4] Lacinilene C (**1**), isolated from the cotton plant *Gossypium hirsutum* L., is an example of a highly oxidized cadinane sesquiterpenoid.[5] Notably, in 2018, lacinilene E (**2**), the benzyl substituted derivative of lacinilene C (**1**), was isolated.[6] More recently, alanenses A (**3**) and B (**4**), C1- and C2-arylated cadinane sesquiterpenoids, were isolated as racemates from the leaves of *Alangium chinense* (Scheme 1A).[7] Importantly, alanenses A and B inhibit spontaneous calcium channel oscillations (SCOs)[8] at low micromolar concentrations. Initial structure–activity relationship studies revealed that the aromatic group at C1- and C2-positions of alanense natural products is essential for the observed inhibitory activity toward SCOs.[7]

We hypothesized that alanense A (**3**) and lacinilene C (**1**) share a common biosynthetic precursor, namely 2,7-dihydroxycadalene (**5**). Previous studies have shown that 2,7-dihydroxycadalene undergoes air oxidation to form lacinilene C (**1**).[9] We proposed that this oxidation involves the reaction of a radical intermediate **6** with triplet oxygen. For the biosynthesis of alanense A (**3**), we speculated that the same radical intermediate (**6**) might instead react with catechol (**7a**). While the biosynthetic pathways of alanense A (**3**) and lacinilene C (**1**) diverge from the radical intermediate **6**, we questioned whether it might be possible to chemically revert lacinilene C (**1**) back to alanense A (**3**). Inspired by recent advancements in deoxygenative

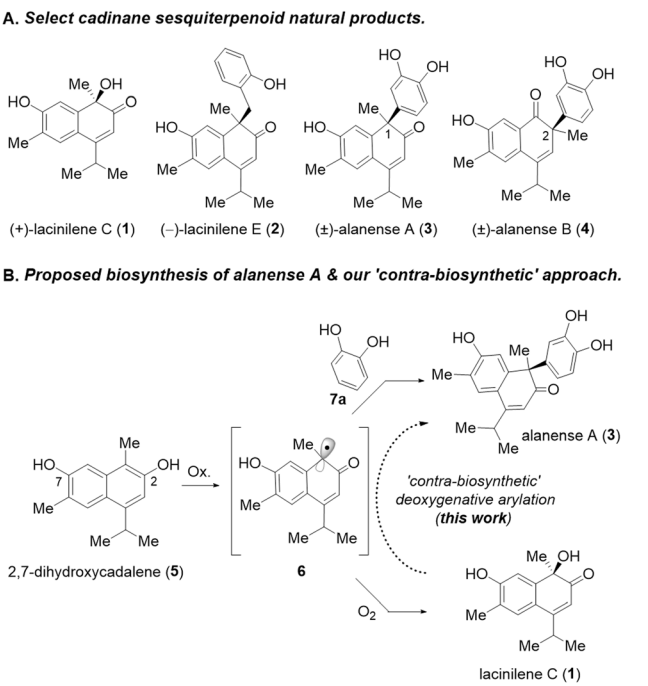

Scheme 1 Our synthetic blueprint towards alanense natural products.

[a]*Department of Chemistry, Korea Advanced Institute of Science and Technology (KAIST), Daejeon 34141, Republic of Korea. E-mail: sunkyu.han@kaist.ac.kr*

[b]*Center for Catalytic Hydrocarbon Functionalizations, Institute for Basic Science (IBS), Daejeon 34141, Republic of Korea*

† Electronic supplementary information (ESI) available: Experimental details including characterization data and NMR spectra. CCDC 2403465, 2403466, 2403461 and 2403468. For ESI and crystallographic data in CIF or other electronic format see DOI: https://doi.org/10.1039/d5sc00341e

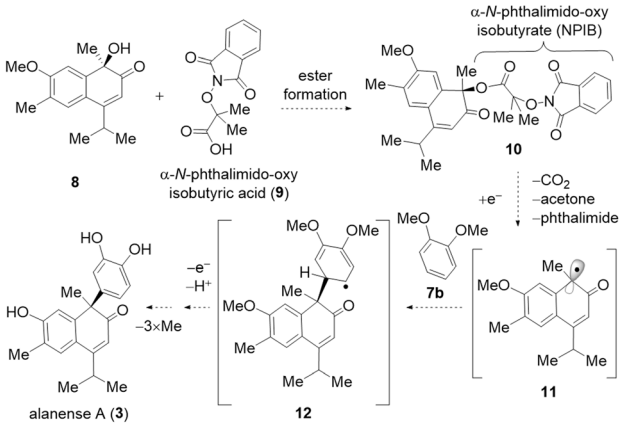

Scheme 2 Our initial synthetic design toward alanense A.

functionalization *via* radical intermediates,[10,11] we envisioned accessing alanense A (**3**) through a deoxygenative arylation[12–17] of lacinilene C (**1**) or its derivative in a "*contra*-biosynthetic" manner (Scheme 1B),[18] intending to use the redox-active ester as a radical precursor.[19]

We recently reported a radical-mediated deoxygenative transformation of tertiary alcohol derivatives to nitriles.[20] The key to success was the development of α-*N*-phthalimido-oxy isobutyrate (NPIB) as a novel redox-active handle for alcohols.[20] We envisioned utilizing the NPIB moiety for the deoxygenative arylation of the lacinilene C derivative as described in Scheme 2. Specifically, we planned to install the NPIB group to the tertiary alcohol moiety of lacinilene C7-methyl ether (**8**). Single-electron transfer (SET) to the NPIB derivative **10** would result in α-carbonyl radical intermediate **11** upon release of phthalimide, carbon dioxide, and acetone (Scheme 2). Radical intermediate **11** was designed to react with catechol derivative **7b** to yield C–C coupled intermediate **12**. SET (oxidation) and deprotonation of radical intermediate **12**, followed by subsequent demethylations of the resulting intermediate, would afford alanense A (**3**).

Results and discussion

Our initial investigations focused on the deoxygenative arylation of NPIB derivative **13a** using $[Ir(dtbbpy)(ppy)_2]PF_6$ as a photoredox catalyst and methanol as a hydrogen bonding-mediated activator of the NPIB moiety.[21] To our delight, when NPIB derivative **13a** was allowed to react with 1,2,4-trimethoxybenzene (**7c**) in the presence of $[Ir(dtbbpy)(ppy)_2]PF_6$ (1 mol%) under 427 nm Kessil lamp irradiation in a methanol/acetonitrile (1 : 2.5, v/v) mixture, arylated product **14a** was isolated in 71% yield (Scheme 3A, entry 1). Notably, when the reaction was conducted without methanol, the product yield was significantly reduced (28%), highlighting the importance of hydrogen bonding-mediated activation of the NPIB moiety (Scheme 3A, entry 2).[21] On the same token, when the reaction was conducted in dimethylformamide (DMF), a strong hydrogen bonding acceptor, product **14a** was obtained in 32% yield consistent with diminished hydrogen bonding activation of the NPIB moiety (Scheme 3A, entry 3). In the absence of light, the reaction was not operative (Scheme 3A, entry 4). Markedly, the addition of BHT to the reaction mixture completely shut down the arylated product formation and resulted in **15** (81% yield) and **16** (40% yield based on the equivalence of NPIB derivative **13a**), consistent with the intermediacy of the radical intermediate (Scheme 3A, entry 5).

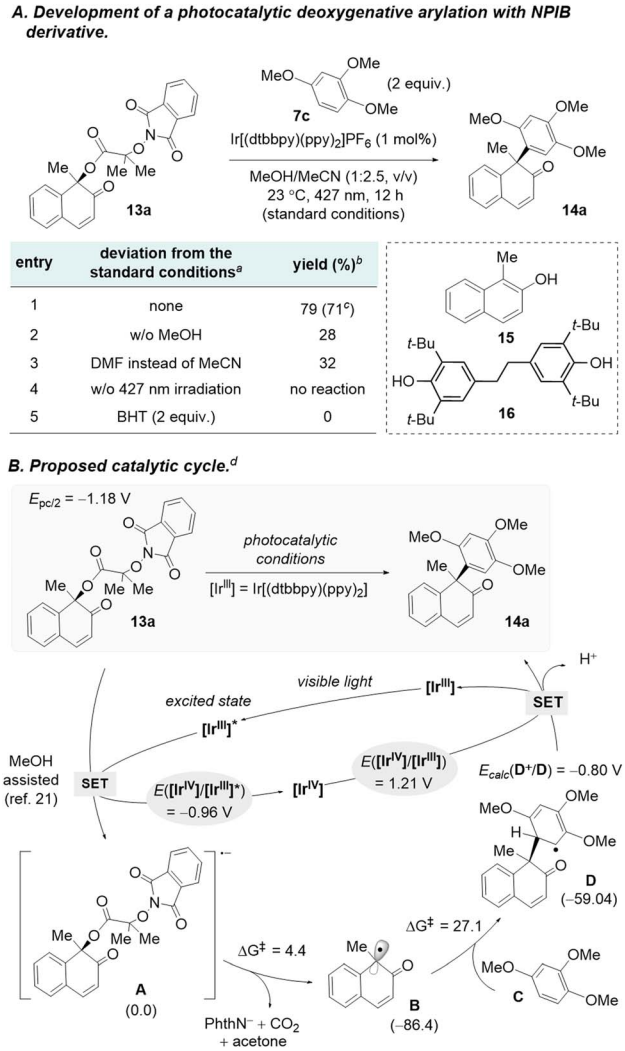

Scheme 3 Development of NPIB-mediated photocatalytic deoxygenative arylation. [a]All reactions were carried out on a 0.1 mmol scale (**13a**) and at 0.2 M. [b]Yields were determined by NMR analysis of the crude reaction mixture using dibromomethane as an internal standard. [c]Isolated yield. [d]Reduction potentials were noted in *V vs.* SCE; computation level = M06-2X/6-311+G** (SMD, solvent = acetonitrile)|M06-2X/6-31G** (SMD, solvent = acetonitrile); unit = kcal mol^{-1}.

Based on our experimental and DFT-calculation results as well as related previous studies,[20,21] we proposed the catalytic cycle depicted in Scheme 3B. Photoexcited $[Ir^{III}]^*$ ($E_{1/2}$ (IV/III*) = −0.96 V *vs.* SCE) species would engage in hydrogen-bond assisted SET with **13a** to produce radical anion **A** which undergoes highly facile fragmentation ($\Delta G^{\ddagger} = 4.4$ kcal mol^{-1}) to deliver electrophilic radical species **B**. The formation of the

radical intermediate **B** was calculated to be a thermodynamically favorable process (−86.4 kcal mol^{-1}), and the subsequent radical addition to **C** is also smooth ($\Delta G^{\ddagger}$ = 27.1 kcal mol^{-1}). The photoredox cycle is then completed by SET between **D** and the oxidizing [Ir^{IV}] species leading to the formation of a cation, which undergoes aromatization to furnish **14a** (for details, see Fig. S2 and S3†).

After developing the NPIB-mediated photocatalytic deoxygenative arylation, we turned our attention to its application in the total synthesis of alanense natural products.[22,23] Our synthesis commenced with a regioselective reverse-prenylation of commercially available aryl iodide **17** using prenylboronic ester **18**[24] in the presence of $Pd(PPh_3)_4$ and CsF[25] to afford coupled product **19** in 46% yield (Scheme 4). With terminal alkene **19** in hand, we then employed Wickens' radical hydrocarboxylation to produce homologated carboxylic acid **20** in 71% yield.[26] Subsequently, carboxylic acid **20** was transformed into cadinane framework **22** based on McCormick's protocol.[27] Epoxidation of compound **22** followed by an oxidative epoxide opening reaction afforded natural 2-hydroxy-7-methoxycadalene (**23**) in 38% yield over two steps.[28] Oxone-mediated dearomatization of naphthol derivative **23** yielded α-hydroxyketone **8** in 58% yield.[29] Esterification of the tertiary alcohol group in compound **8** with α-*N*-phthalimido-oxy isobutyric acid (**9**) was achieved in 82% yield in the presence of EDC·HCl and DMAP. With NPIB derivative **10** in hand, the stage was set for the deoxygenative arylation reaction. However, an intractable mixture of products was observed when NPIB derivative **10** and 1,2-dimethoxybenzene (**7b**) were subjected to the aforementioned standard photoredox catalytic conditions (Scheme 4).

We speculated that the increased electron density of the α-keto radical intermediate and the decreased electron density of the aromatic coupling partner caused a polarity mismatch during the key C–C bond formation. In fact, DFT calculations revealed that the activation barrier for the C–C coupling between radical intermediate **B** (Scheme 3B) and 1,2,4-trimethoxybenzene is 27.1 kcal mol^{-1}, while the activation energy for the coupling between radical **11** and 1,2-dimethoxybenzene is 32.4 kcal mol^{-1} (for details, see Fig. S4†). Extensive experimentations were conducted with a model system to remedy the observed lack of desired reactivity under our previously optimized photocatalytic reaction conditions. To our delight, we discovered that NPIB derivative **10** and 1,2-dimethoxybenzene (**7b**) could be coupled in the presence of 5 equiv. of TFA in hexafluoroisopropanol (HFIP) to yield product **24** in 98% yield (*vide infra*). It is noteworthy that the carbocationic moiety is efficiently formed at the α-position of the ketone from the NPIB group under the newly discovered optimized reaction conditions. Finally, treatment of trimethylated compound **24** with 10 equiv. of BBr_3 afforded the synthetic sample of alanense A (**3**) in 59% yield.

The optimization studies of the key NPIB-mediated Friedel–Crafts-type arylation are shown in Scheme 5. Treatment of NPIB derivative **13a** and 2,3,6-trimethylphenol (**7d**, 2 equiv.) with TFA (5 equiv.) in HFIP solution produced deoxygenative arylated product **14b** in 80% isolation yield along with α-*N*-phthalimido-oxy isobutyric acid **9** (Scheme 5, entry 1). The use of HFIP as a solvent was critical as the reaction did not proceed when acetonitrile, DMF, tetrahydrofuran, methylene chloride, or methanol were employed as a solvent (Scheme 5, entries 2–6).[30,31] TFA was the optimal acid for the reaction since other Brønsted acids such as formic acid or acetic acid resulted in full recovery of NPIB derivative **13a** (Scheme 5, entries 7 and 8). When stronger triflic acid was employed, NPIB derivative **13a** underwent undesired decomposition leading to only 4% of coupled product **14b** (Scheme 5, entry 9). In the absence of TFA, the reaction did not proceed at all (Scheme 5, entry 10). The use of 1 or 3 equiv. of TFA resulted in lower product yields due to slower conversion (Scheme 5, entries 11 and 12). The reaction proceeded in the dark, indicating that the mechanism does not involve a photoinduced radical pathway (Scheme 5, entry 13).

Next, the reactivity of the NPIB group was compared with that of other leaving groups. When hydroxyl derivative **13b** was

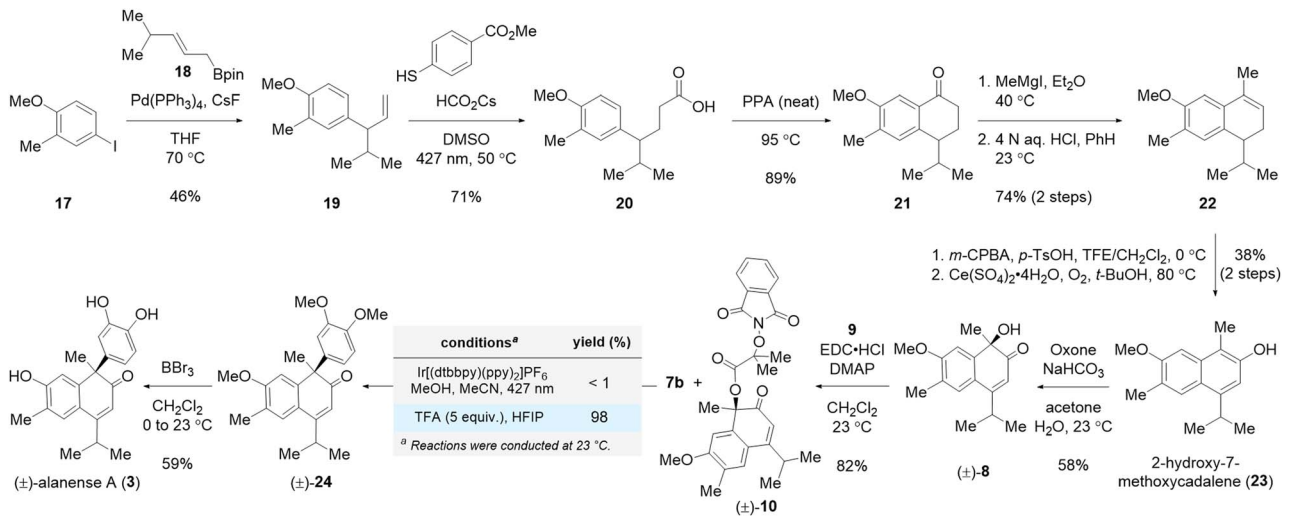

Scheme 4 Total synthesis of alanense A.

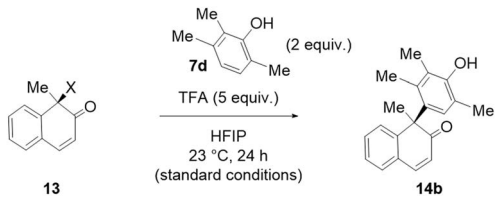

entry	substrate	deviation from the standard conditions[a]	yield (%)[b]
1	**13a** (X = NPIB)	none	84 (80[c])
2	**13a**	MeCN instead of HFIP	no reaction
3	**13a**	DMF instead of HFIP	no reaction
4	**13a**	THF instead of HFIP	no reaction
5	**13a**	CH_2Cl_2 instead of HFIP	no reaction
6	**13a**	MeOH instead of HFIP	no reaction
7	**13a**	HCOOH instead of TFA	no reaction
8	**13a**	AcOH instead of TFA	no reaction
9	**13a**	TfOH instead of TFA	4
10	**13a**	TFA (0 equiv.)	no reaction
11	**13a**	TFA (1 equiv.)	43
12	**13a**	TFA (3 equiv.)	74
13	**13a**	in the dark	82
14	**13b** (X = OH)	none	22
15	**13c** (X = OAc)	none	26
16	**13d** (X = OPiv)	none	4
17	**13e** (X = OBz)	none	12
18	**13f** (X = $O(CO)_2OMe$)	none	13
19	**13g** (X = Br)	none	0
20	**13a**	standard photocatalytic conditions developed in Scheme 3	4

Scheme 5 Optimization of the acid-mediated deoxygenative arylation. [a]All reactions were carried out on a 0.1 mmol scale (**13a–13g**) and at 0.25 M. [b]Yields were determined by NMR analysis of the crude reaction mixture using 1,3,5-trimethoxybenzene as an internal standard. [c]Isolated yield.

employed as a substrate under the optimized reaction conditions, the desired arylated product **14b** was obtained in 22% yield (Scheme 5, entry 14).[32,33] Other carboxylate-based leaving groups, such as acetate (**13c**), pivalate (**13d**), benzoate (**13e**), and methyl oxalate (**13f**) exhibited lower yields compared to the NPIB group (Scheme 5, entries 15–18), indicating the superior leaving group ability of NPIB (for details, see Fig. S6†). Even though the product yields were lower, the formation of the coupled product **14b** with these leaving groups suggests the involvement of a carbocation intermediate. Subjection of bromide derivative **13g** under the optimized reaction conditions did not yield the desired coupled product (Scheme 5, entry 19) and only reduced product **15** and 4-bromo-2,3,6-trimethylphenol were observed. Under the standard photocatalytic deoxygenative arylation conditions, a 4% yield of the coupled product was observed. The lower O–H bond dissociation energy of the phenol moiety facilitated a hydrogen atom transfer to the radical intermediate, leading to the formation of **15**, which was obtained in 81% yield, along with 28% of the oxidative dimer of the phenol derivative **7d** (Scheme 5, entry 20).

With the reaction conditions for acid-mediated deoxygenative arylation in hand, we hypothesized that the reaction may proceed *via* protonation-mediated NPIB dissociation followed by the Friedel–Crafts-type arylation process. Indeed, the formation of α-*N*-phthalimido-oxy isobutyric acid **9** was observed experimentally, supporting this mechanistic proposal. To further evaluate its plausibility, we conducted DFT calculations (Fig. 1). As expected, subsequent processes including protonation of **13a** to form **[13a-H]**, intramolecular proton transfer providing **[13a-H]′**, and dissociation of **9** to furnish carbocationic intermediate **B′** were found to be kinetically accessible at room temperature ($\Delta G^{\ddagger}$ = 21.5 kcal mol^{-1}) although they are slight endergonic processes (ΔG = 7.3 kcal mol^{-1}). Consequently, the Friedel–Crafts-type reaction with **B′** and electron rich aryl substrate **C′** to provide C–C coupled intermediate **D′** also turned out to be thermodynamically and kinetically plausible (ΔG = −5.3 kcal mol^{-1} and $\Delta G^{\ddagger}$ = 2.5 kcal mol^{-1}). As a final step, highly exergonic deprotonation of **D′** can provide the observed corresponding deoxygenative arylation product **14b** (ΔG = −40.2 kcal mol^{-1}).

With the two standard conditions established for NPIB-mediated deoxygenative arylations, the substrate scope was first investigated under photocatalytic conditions (Fig. 2, conditions A). Nitrogen-containing arenes participated in the reaction, affording arylated products (**14c** and **14d**). Notably, acid- and/or base-sensitive functional groups on the arene, such as Boc (**14c**), MOM (**14e**), Bn (**14f**), and silyl (**14g** and **14h**), were compatible with the reaction conditions. The substrate with the NPIB moiety juxtaposed between two carbonyl groups produced the arylated product **14ah** in 41% yield. However, arylated products were obtained only from electron-rich 1,2,4-tri-substituted arenes.

Next, the substrate scope of aryl coupling partners was investigated under acidic conditions (Fig. 2, conditions B).

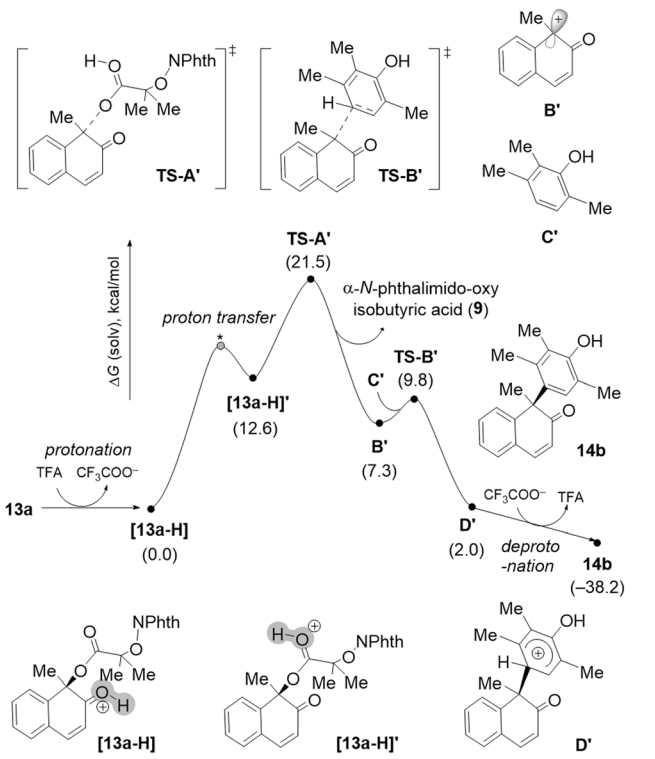

Fig. 1 Gibbs free energy profiles for the acid-mediated deoxygenative arylation mechanism.

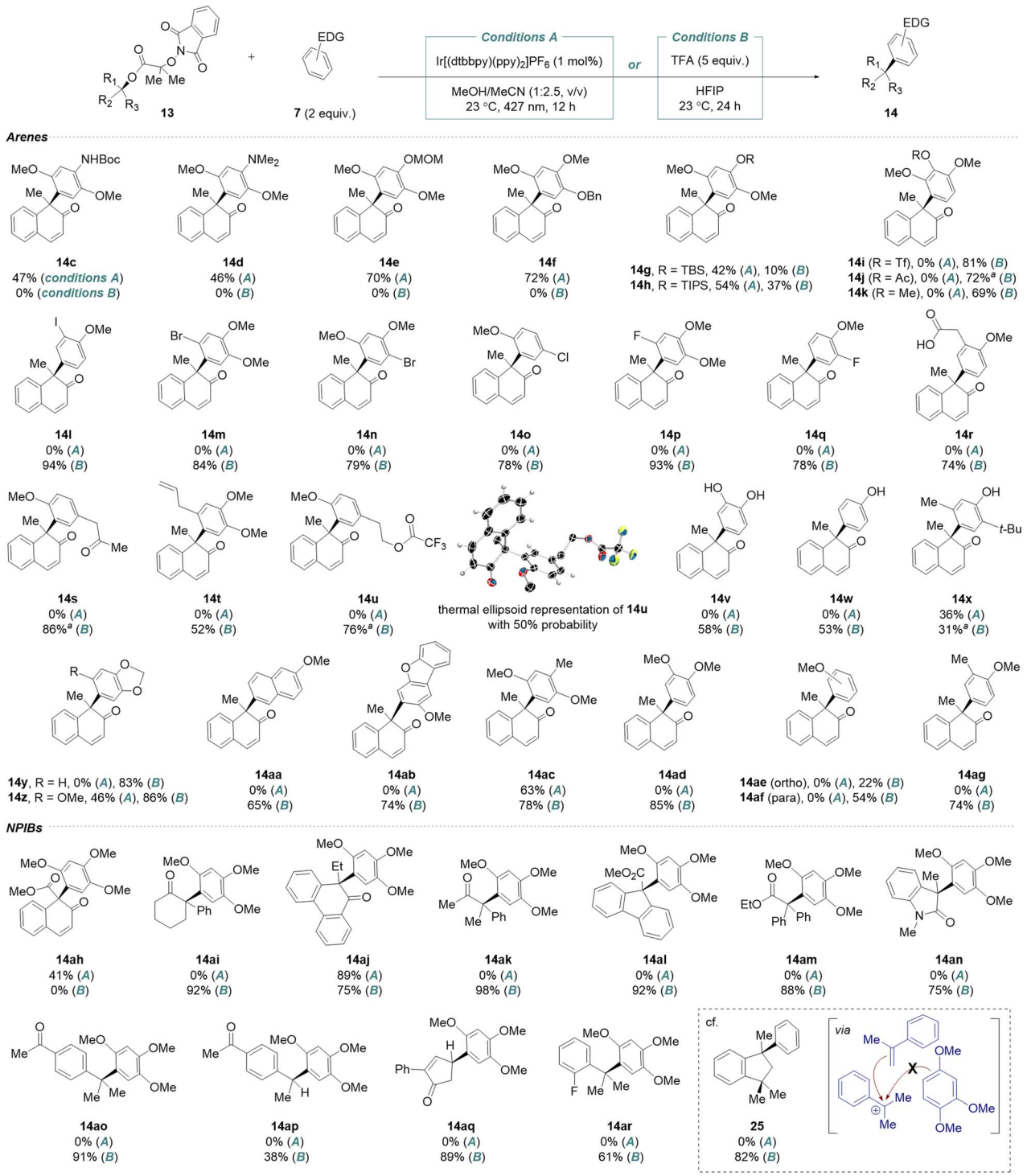

Fig. 2 Substrate scope of the NPIB-mediated arylation reaction. All reactions were carried out on a 0.1 mmol scale and at 0.25 M. [a]TFA (20 equiv.) was used.

Triflate (**14i**), acetate (**14j**), iodide (**14l**), bromide (**14m** and **14n**), chloride (**14o**), and fluoride (**14p** and **14q**) groups were compatible with our newly discovered reaction conditions. It is noteworthy that the presence of inductively electron-withdrawing halides did not hamper the reaction outcomes. The carboxylic acid, ketone and terminal olefin groups were compatible under the standard reaction conditions (**14r–14t**). The substrate with a primary hydroxyl group could be employed in our coupling reaction conditions. In this case, the hydroxyl group underwent trifluoroacetylation (**14u**). The phenolic moiety, which was problematic under the previously described photocatalytic reaction conditions, was compatible under the

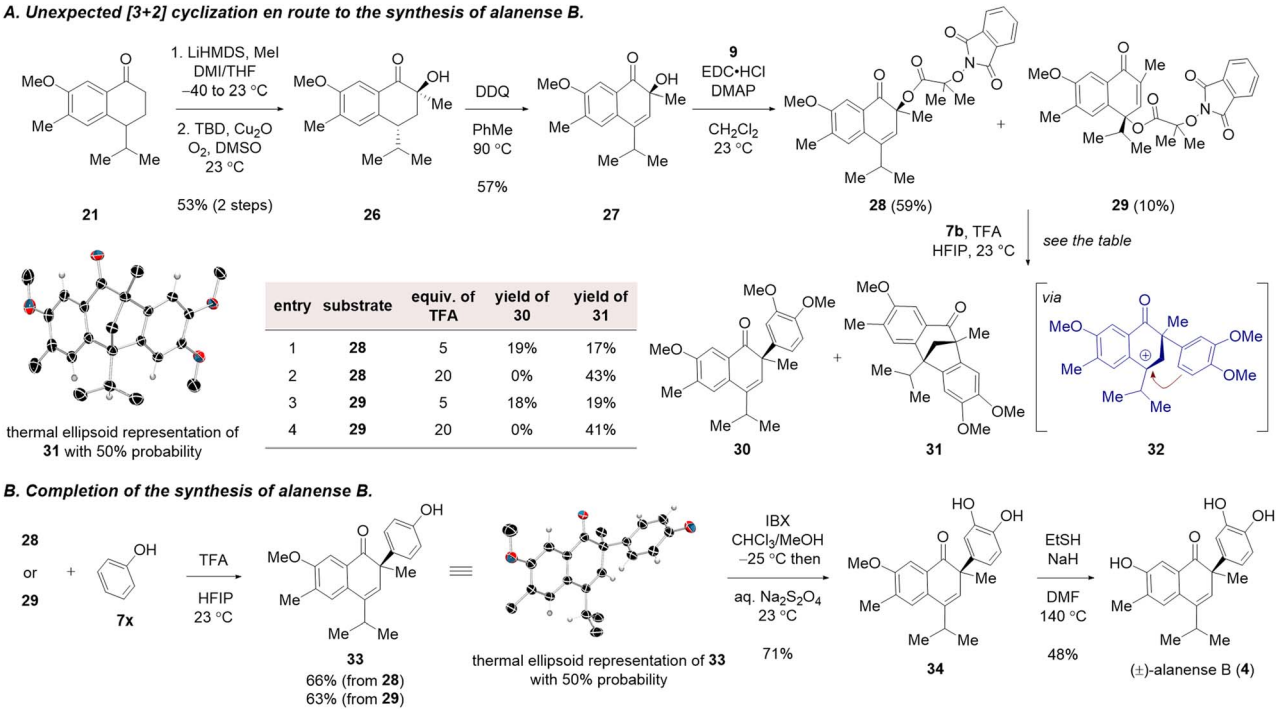

Scheme 6 Total synthesis of alanense B.

optimized TFA + HFIP reaction conditions (**14v–14x**). Bicyclic (**14y–14aa**) and tricyclic (**14ab**) aromatic systems yielded the coupled products in good yields. Notably, when anisole was employed as a coupling partner, *ortho*- and *para*-regioisomers were obtained in 22% (**14ae**) and 54% (**14af**) isolation yields, respectively. It is noteworthy that for all other cases delineated here, products were obtained as a single regioisomer. Unlike under photocatalytic conditions, no arylated products were obtained from nitrogen-containing arenes (**14c** and **14d**) or those bearing Boc (**14c**), MOM (**14e**), or Bn (**14f**) groups. Additionally, silyl groups (**14g** and **14h**) were not well tolerated.

We subsequently surveyed the scope of NPIB derivatives under acidic conditions. Structurally diverse benzylic and tertiary NPIB derivatives yielded coupling products with 1,2,4-trimethoxybenzene in good yields. The presence of an ester (**14al** and **14am**) or an amide moiety (**14an**) at the α-position of NPIB did not hinder the reaction. As long as the ketone group is conjugated to the carbon attached to the NPIB group either *via* an aromatic ring (**14ao** and **14ap**) or an olefin (**14aq**), the arylated products were formed in moderate to good yield. Notably, secondary NPIB derivatives were successfully transformed into arylated products under the standard reaction conditions (**14ap** and **14aq**). Interestingly, when the NPIB derivative of 2-phenylpropan-2-ol was subjected to the standard reaction conditions, homodimerization product **25** was formed in 82% yield. It is reasoned that the benzylic carbocationic intermediate is trapped with *in situ* generated α-methylstyrene. When an analogous NPIB derivative with an *ortho*-fluoride moiety at the phenyl group was employed, the desired arylated product (**14ar**) was obtained in 61% yield. Unlike under photocatalytic conditions, the formation of a carbocation at the 1,3-diketone moiety proved challenging, preventing the formation of the desired product (**14ah**).

We next embarked on the total synthesis of alanense B (**4**). α-Methylation of common ketone precursor **21** and subsequent α-hydroxylation of the resulting methylated product *via* a protocol reported by the Schoenebeck group[34] afforded alcohol **26** in 53% yield over two steps (Scheme 6). Oxidation of compound **26** with DDQ produced conjugated alcohol **27** in 57% yield. Treatment of alcohol **27** with NPIB acid **9** in the presence of EDC·HCl and DMAP forged NPIB derivative **28** as a single regioisomer. However, NPIB derivative **28** was partially isomerized to **29** during silica gel column chromatography to yield **28** and **29** in 59% and 10% yield, respectively. Interestingly, treatment of **28** with 1,2-dimethoxybenzene (**7b**) and 5 equiv. of TFA in HFIP solution yielded desired arylated product **30** (19%) along with [3+2] cycloaddition product **31** (17%), likely formed *via* cationic intermediate **32**. When **28** was allowed to react with 20 equiv. of TFA in HFIP, only cycloaddition product **31** was obtained in 43% yield. The structure of [3+2] cycloaddition product **31** was unambiguously confirmed by a single crystal X-ray diffraction analysis. It is notable that the bicyclo[3.2.1]octadienone framework in **31** constitutes the backbone of various natural products including naphthocyclinone.[35] The subjection of the NPIB regioisomer **29** to these reaction conditions revealed analogous reaction outcomes.

To circumvent the formation of the [3+2] cycloaddition byproduct, phenol (**7x**) was selected as the coupling partner. We reasoned that the undesired intramolecular Friedel–Crafts reaction-based cyclization would not be feasible because the *meta* position of the phenol group is deactivated by an inductively electron-withdrawing oxygen atom. This strategic design

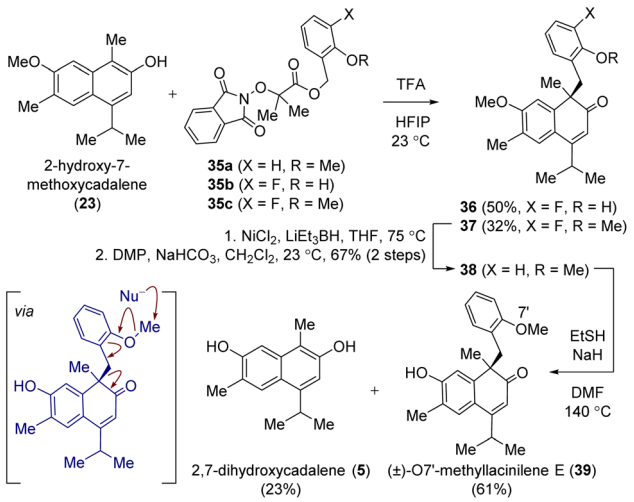

Scheme 7 Synthesis of the core of lacinilene E.

was possible owing to the broad substrate scope of the newly developed TFA/HFIP-based arylation reaction. In the event, when NPIB derivative **28** (or **29**) was allowed to react with phenol in the presence of TFA (5 equiv.) in HFIP, the desired α-arylated product **33** was exclusively formed in 66% yield (63% yield from **29**). The exclusive arylation at the α-position of the ketone group is noteworthy. Based on DFT calculations, nucleophilic phenol addition at the α-position is kinetically favored ($\Delta G^{\ddagger} = 14.5$ kcal mol^{-1}) over addition at the benzylic position ($\Delta G^{\ddagger} = 17.2$ kcal mol^{-1}), presumably due to the significant steric hindrance posed by the benzylic isopropyl substituent (for details, see Fig. S7†).

For the endgame of the synthesis, phenol derivative **33** was oxidized to the *ortho*-quinone derivative in the presence of IBX at −25 °C. Subsequent one-pot addition of aqueous sodium dithionite solution to the reaction mixture resulted in catechol derivative **34** in 71% yield. The use of chloroform/methanol co-solvent was critical for the efficient transformation.[36] The final demethylation of the methoxy group in **34** was achieved by treating it with ethanethiol and sodium hydride in DMF to produce the first synthetic sample of alanense B (**4**) in 48% yield.

Finally, we envisioned applying the newly developed NPIB-based deoxygenative transformation into the synthesis of lacinilene E (**2**) (Scheme 7). To this end, 2-hydroxy-7-methoxycadalene (**23**) was allowed to react with NPIB derivative **35a** in the presence of TFA in HFIP. However, only the decomposition of NPIB derivative **35a** was observed under these reaction conditions. We speculated that the electron-rich NPIB derivative **35a** acts as a dominant nucleophile over 2-hydroxy-7-methoxycadalene (**23**). To temper the nucleophilic reactivity of the NPIB derivative, we designed fluorinated NPIB derivatives **35b** and **35c**. To our delight, when **23** was allowed to react with fluorinated NPIB derivatives **35b** and **35c** in the presence of TFA in HFIP, coupled products **36** and **37** were formed in 50% and 32% yield, respectively. $NiCl_2$-catalyzed hydrodefluorination using superhydride as a reductant[37] afforded the defluorinated allylic alcohol product from compound **37**. Subsequent DMP-mediated oxidation of the resulting alcohol resulted in dimethylated lacinilene E derivative **38** (67% yield over two steps). Markedly, the defluorinated product of compound **36** was not observed under the various conditions tested. Demethylation at the O7′ position of compound **38** was extremely challenging. 2,7-dihydroxycadalene (**5**) was obtained as a major product under various demethylation conditions used. We reasoned that the demethylation at O7′ induced the C–C bond cleavage *via* the formation of an *ortho*-quinone methide. In fact, when compound **38** was reacted with boron tribromide as a demethylating agent, a trace amount of lacinilene E (**2**) was obtained along with 2,7-dihydroxycadalene as a major product (for details, see Fig. S1†). Subjection of compound **38** to ethanethiol and sodium hydride in DMF delivered the methylated congener O7′-methyllacinilene E (**39**) in 61% yield along with 2,7-dihydroxycadalene (**5**) in 23% yield.

Conclusions

In conclusion, we have completed the total synthesis of alanenses A and B. To achieve the biosynthetically inspired[38,39] arylation, we designed deoxygenative arylation reactions of α-hydroxycarbonyl derivatives. By utilizing α-*N*-phthalimido-oxy isobutyrate (NPIB) as a redox-active handle for hydroxyl groups, we have established a photoredox-catalyzed deoxygenative arylation reaction that proceeds *via* radical intermediates. Although challenges arose when applying this photocatalytic approach to the synthesis of alanense A, we overcame these obstacles by developing an alternative method using TFA/HFIP, which enabled the arylation of the NPIB derivative *en route* to the target natural products. Notably, our work demonstrated that the combination of the NPIB group with TFA and HFIP effectively promotes Friedel–Crafts reactions, even in the challenging context of generating carbocations adjacent (or conjugated) to electron-withdrawing groups such as carbonyl moieties. This methodology enabled streamlined total syntheses of alanenses A, B, and O7′-methyllacinilene E. Ongoing studies aim to further explore and expand the versatile reactivity of the NPIB group, with findings to be presented in future reports.

Data availability

The experimental procedures and additional data can be found in the ESI.† Crystallographic data for the structure reported in this article have been deposited at the Cambridge Crystallographic Data Centre, under deposition numbers 2403465 (**14u**), 2403466 (**26**), 2403461 (**31**), and 2403468 (**33**). Copies of the data can be obtained free of charge from the CCDC *via* **https://www.ccdc.cam.ac.uk/structures/**.

Author contributions

Y. E. H. and S. H. conceived the study and obtained funding. S. H. supervised the project. Y. E. H. played a key role in the experimentation. J. K. carried out computational studies. T.

H. L. P. investigated the substrate scope. D. K. performed the single crystal X-ray diffraction analysis. Y. E. H., J. K. and S. H. wrote the manuscript.

Conflicts of interest

There are no conflicts to declare.

Acknowledgements

This research was supported by the Basic Science Research Program through the National Research Foundation of Korea (NRF) funded by the Ministry of Education (2019R1A6A1A10073887). This work was also supported by the National Research Foundation of Korea (NRF-2021R1A2C2011203), KAIST Grand Challenge 30 project, and KAIST Cross-Generation Collaborative Lab Project.

References

1 D. W. Christianson, *Chem. Rev.*, 2017, **117**, 11570–11648.
2 I. Pateraki, A. M. Heskes and B. Hamberger, *Adv. Biochem. Eng./Biotechnol.*, 2015, **148**, 107–139.
3 X.-Y. Chen, Y. Chen, P. Heinstein and V. J. Davisson, *Arch. Biochem. Biophys.*, 1995, **324**, 255–266.
4 C. A. Citron, J. Gleitzmann, G. Laurenzano, R. Pukall and J. S. Dickschat, *Chembiochem*, 2012, **13**, 202–214.
5 R. D. Stipanovic, P. J. Wakelyn and A. A. Bell, *Phytochemistry*, 1975, **14**, 1041–1043.
6 Y.-G. Xie, S.-l. Zhu, Y.-y. Huang, Y.-g. Guo, G.-j. Wu, I. Muhammad, S.-k. Yan, H.-z. Jin and W.-d. Zhang, *Phytochem. Lett.*, 2018, **28**, 64–68.
7 C.-L. Zhang, J. Liu, C.-C. Xi, Y.-G. Cao, J. He, S.-C. Li, F. Zhang, C. B. Naman and Z.-Y. Cao, *J. Nat. Prod.*, 2022, **85**, 599–606.
8 X.-s. Wang and E. I. Gruenstein, *Brain Res.*, 1997, **767**, 239–249.
9 R. D. Stipanovic, G. A. Greenblatt, R. C. Beier and A. A. Bell, *Phytochemistry*, 1981, **20**, 729–730.
10 T. Mandal, S. Mallick, M. Islam and S. De Sarkar, *ACS Catal.*, 2024, **14**, 13451–13496.
11 A. Cook and S. G. Newman, *Chem. Rev.*, 2024, **124**, 6078–6144.
12 Z. Dong and D. W. C. MacMillan, *Nature*, 2021, **598**, 451–456.
13 X. Zhang and D. W. C. MacMillan, *J. Am. Chem. Soc.*, 2016, **138**, 13862–13865.
14 L. Reginald Mills, J. J. Monteith, G. dos Passos Gomes, A. Aspuru-Guzik and S. A. L. Rousseaux, *J. Am. Chem. Soc.*, 2020, **142**, 13246–13254.
15 W. Xu, C. Fan, X. Hu and T. Xu, *Angew. Chem., Int. Ed.*, 2024, **63**, e202401575.
16 S. K. Jana, R. Bhattacharya, P. Dey, S. Chakraborty and B. Maji, *ACS Catal.*, 2024, **14**, 14172–14182.
17 E. C. Gentry, L. J. Rono, M. E. Hale, R. Matsuura and R. R. Knowles, *J. Am. Chem. Soc.*, 2018, **140**, 3394–3402.
18 M. A. Hardy, J. Hayward Cooke, Z. Feng, K. Noda, I. Kerschgens, L. A. Massey, D. J. Tantillo and R. Sarpong, *Angew. Chem., Int. Ed.*, 2024, **63**, e202317348.
19 Z. Huang and J.-P. Lumb, *Nat. Chem.*, 2021, **13**, 24–32.
20 S. Lee, G. Kang and S. Han, *Org. Lett.*, 2024, **26**, 5640–5645.
21 A. Tlahuext-Aca, R. A. Garza-Sanchez and F. Glorius, *Angew. Chem., Int. Ed.*, 2017, **56**, 3708–3711.
22 K. Makino, R. Fukuda, S. Sueki and M. Anada, *J. Org. Chem.*, 2024, **89**, 2050–2054.
23 M. Kadarauch, T. A. Moss and R. J. Phipps, *J. Am. Chem. Soc.*, 2024, **146**, 34970–34978.
24 Y. T. Boni, J. Vaitla and H. M. L. Davies, *Org. Lett.*, 2023, **25**, 5–10.
25 S. Kotha, M. Behera and V. Shah, *Synlett*, 2005, **12**, 1877–1880.
26 S. N. Alektiar, J. Han, Y. Dang, C. Z. Rubel and Z. K. Wickens, *J. Am. Chem. Soc.*, 2023, **145**, 10991–10997.
27 J. P. McCormick, T. Shinmyozu, J. Paul Pachlatko, T. R. Schafer, J. W. Gardner and R. D. Stipanovic, *J. Org. Chem.*, 1984, **49**, 34–40.
28 Y. Zhang, Y. Liao, X. Liu, X. Xu, L. Lin and X. Feng, *Chem. Sci.*, 2017, **8**, 6645–6649.
29 M. J. Cabrera-Afonso, M. Carmen Carreño and A. Urbano, *Adv. Synth. Catal.*, 2019, **361**, 4468–4473.
30 I. Colomer, A. E. R. Chamberlain, M. B. Haughey and T. J. Donohoe, *Nat. Rev. Chem.*, 2017, **1**, 0088.
31 K. Morimoto, K. Sakamoto, Y. Ohnishi, T. Miyamoto, M. Ito, T. Dohi and Y. Kita, *Chem.–Eur. J.*, 2013, **19**, 8726–8731.
32 A. Kumar, T. V. Singh, S. P. Thomas and P. Venugopalan, *Eur. J. Org Chem.*, 2020, **2020**, 2530–2536.
33 L. Chen and J. Zhou, *Chem.–Asian J.*, 2012, **7**, 2510–2515.
34 A. S.-K. Tsang, A. Kapat and F. Schoenebeck, *J. Am. Chem. Soc.*, 2016, **138**, 518–526.
35 Y. Ando, T. Hoshino, N. Tanaka, M. M. Maturi, Y. Nakazawa, T. Fukazawa, K. Ohmori and K. Suzuki, *Angew. Chem., Int. Ed.*, 2025, **64**, e202415108.
36 A. Pezzella, L. Lista, A. Napolitano and M. d'Ischia, *Tetrahedron Lett.*, 2005, **46**, 3541–3544.
37 J. Wu and S. Cao, *ChemCatChem*, 2011, **3**, 1582–1586.
38 G. Kang and S. Han, *Bull. Korean Chem. Soc.*, 2024, **45**, 876–879.
39 R. C. Godfrey, H. E. Jones, N. J. Green and A. L. Lawrence, *Chem. Sci.*, 2022, **13**, 1313–1322.